DOI 10.1007/s10946-020-09893-7
Journal of Russian Laser Research, Volume 41, Number 4, July, 2020

IMAGING RESEARCH OF TWO-DIMENSIONAL PHOTONIC-CRYSTAL FLAT LENS WITH HEXAGONAL STRUCTURE

Jian Lu[1*] and YanRong Zhang[2]

[1] *Public Experiment Center*
University of Shanghai for Science and Technology
Shanghai 200093, China

[2] *Vocational Education College*
Anyang University
Anyang 455000, China

*Corresponding author e-mail: jianlu@usst.edu.cn

Abstract

Based on the finite-difference-time-domain method and the plane-wave method, we study the imaging performance of two-dimensional hexagonal-structure photonic-crystal flat panel lens. First, the plane wave expansion method is used to verify that the structure has a negative refraction effect. The equivalent refractive index is -1 when the normalized frequency is 0.251. The finite-difference-time-domain method is used to study the imaging performance of the structure for the small circular target (radius 1/12 wavelength). The simulation result shows that the imaging resolution of the target is greatly improved by a photonic-crystal flat lens with hexagonal structure. Then the side length of square air hole is changed to study the influence on the imaging performance. We find that the imaging resolution is different for different side lengths. The general trend is that the imaging resolution gradually increases, when the side length of hole increases (from $0.1\,a$ to $0.5\,a$). There is an optimum resolution when the side length is $0.5\,a$. The result shows that the imaging performance of the lens can be optimized by changing the side length of holes. It provides a theoretical basis for the practical application of the photonic-crystal flat lens.

Keywords: photonic crystal, negative refraction, hexagonal structure, flat lens, imaging.

1. Introduction

Lens is the most basic component in an optical system. Conventional lens is formed by a transparent medium surrounding with two refractive curved surfaces. The position of main optical axis, focus, and focal length are determined, when the surface of the lens is determined. The image resolution of conventional lens is constrained by the diffraction limit, because most phase information is lost. Negative refractive material with negative permeability and permittivity [1], as a new type of artificial electromagnetic material, has attracted great research interest in recent years. Negative refractive material is also called the left-handed material (LHM), since the electric field, the magnetic field, and the wave vector satisfy the left-handed spiral relationship.

The appearance of "perfect lens" [2] based on negative refractive material solves the flaw of the traditional lens. Since the "perfect lens" is a flat lens, the processing procedure is relatively simple. Most

Manuscript submitted by the authors in English first on May 15, 2020 and in final form on June 1, 2020.

phase information retained, when the light wave passes through the lens. The imaging by the "perfect lens" will not be restricted by the diffraction limit, enabling sub-wavelength imaging, which is higher than conventional lenses [3–7].

It is regrettable that negative refractive material does not exist in nature. Smith et al. [8, 9] found that negative refraction phenomena exit in the periodic structure composed of metal columns. But the applications are limited, because the energy is greatly absorbed in the periodic structure of metal components. Photonic crystals (PCs) [10, 11] are considered because photonic crystals may have own equivalent negative refraction effects; they are easily to implement.

Photonic crystals are highly modulatable, and the development of optical photonic-crystal lenses with equivalent negative refractive properties will make a significant advancement in optical imaging systems. Thus, a negative-refractive photonic-crystal (abbreviated as NR-PC) flat lens [12,13] is produced, and the imaging of the NR-PC flat lens follows geometric optical characteristics [14, 15]; thus, it can be applied to the light-wave target detection and imaging systems.

Photonic crystal is an artificial material whose dielectric constant changes periodically, and it can control light transmission simply and efficiently. Due to the negative refraction effect, when the light wave is incident on the NR-PC flat lens, the incident light and the refracted light are no longer separated on both sides of the normal but on the same side of the normal. The NR-PC flat lens achieves sub-wavelength imaging that breaks through the diffraction limit. The lens is not limited by the paraxial condition and can amplify the evanescent wave, thereby significantly improving the image quality. The equivalent negative refractive index of a photonic crystal can be adjusted by the dielectric constant and periodicity of the material, and the electromagnetic loss at high frequencies is little, so NR-PC is easier to implement in the infrared and optical fields than the left-handed material.

2. Numerical Simulation

The research in this paper is based on the plane-wave expansion method and the finite-difference-time-domain method. The plane-wave expansion method [16] is a frequency-domain calculation method, which was first proposed and applied more commonly. The Maxwell equations in the periodic-structure medium are converted into the eigenvalue problem of the frequency to solve. This method is applicable to the eigenmodes of any periodic structure. The idea is to use the Bloch theorem [17] to spread the electric or magnetic field with a plane wave and transform the Maxwell equations from the time domain to the discrete Fourier space, so that the calculation of the energy band is simplified to solve the eigenvalue problem of algebra.

The finite-difference-time-domain method was proposed by K. Yee in 1966 [18] and can simulate the dynamic process of electromagnetic waves responding in different structures. Originally the method was used to deal with the propagation and reflection of electromagnetic pulses; now it has been applied widely. The finite-difference-time-domain method can directly solve the time-varying curl equation of the Maxwell equations and replace all the derivation of the space coordinate system and time with a series of finite difference expressions. The method can also directly solve the magnetic-field and electric-field amplitude distributions of the target structure in time domain; it is suitable for electromagnetic field analysis of almost all kinds of components. At the same time, the finite-difference-time-domain method can intuitively describe the process of electromagnetic field changes in space. In this paper, we apply the finite-difference-time-domain method to the numerical simulation of the electromagnetic wave propagation in photonic crystals. The boundary condition used in the calculation is the perfect matching

layer (PML) [19].

The photonic-crystal band gap is calculated by the plane-wave method, while the field strength distribution is calculated by the finite-difference-time-domain method.

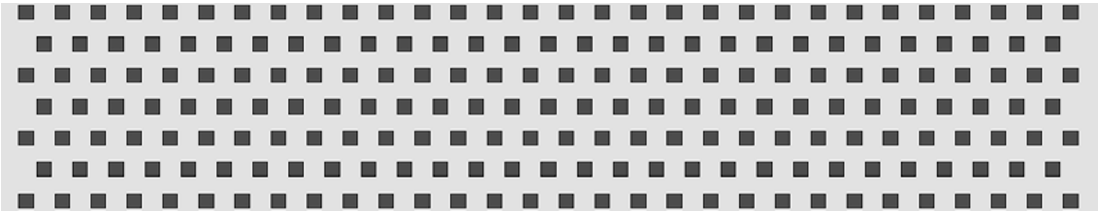

Fig. 1. Schematic diagram of a two-dimensional hexagonal-square-hole photonic-crystal flat lens.

In this paper, we consider a two-dimensional photonic-crystal plate model with hexagonal structure. The hexagonal type of graphene structure is a honeycomb lattice, which is formed by removing some holes on the basis of a two-dimensional triangle. It is composed of etching a square hole on a gallium arsenide (GaAs) dielectric substrate, and the holes are arranged in a triangular pattern periodically (horizontal one behavior 30, and one behavior 29 air holes staggered, vertical direction 7 rows). On this basis, some air holes are removed from the center (the hexagonal array of honeycomb lattice is shown in Fig. 1), and the smallest unit cell is hexagonal. It is considered to be infinitely long in the Y direction. The side length of the square air hole is $0.4\,a$ ($a = 1$ μm is the lattice constant of the two-dimensional triangular-lattice photonic crystal), and the dielectric constant of the background material GaAs is $\varepsilon = 12.96$.

The equivalent negative refraction of a photonic crystal used a Bragg multiple scattering of a periodic structure, which wave vector and group velocity are opposite; see Fig. 2 where the abscissa is the value of the wave vector along the boundary of the simple Brillouin zone, starting from the point of Γ. The band-gap structure of TM wave can be calculated by the plane-wave expansion method. The curve in Fig. 2 represents the dispersion curve of air, and the ordinate is the normalized frequency ($f = \omega a/2\pi c = a/\lambda$), where ω is the angular frequency, c is the speed of light in vacuum, and λ is the wavelength of electromagnetic waves.

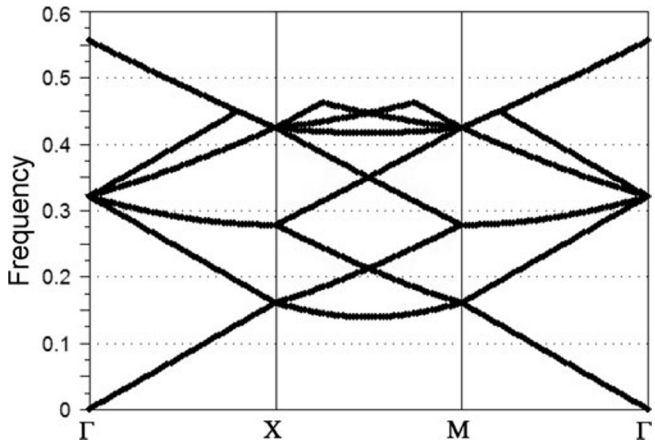

Fig. 2. The TM mode band structure of two-dimensional hexagonal-square flat lens; here, frequency $\omega a/2\pi c = a/\lambda$.

One can see in Fig. 2 that the normalized frequency of the point of Γ is the highest when the normalized frequency f is between 0.15 and 0.32, which means that the gradient direction of the EFS is pointing to the Γ in this frequency range, so that it can be generated negative refraction in this frequency range. More importantly, for the model discussed in this paper, when the normalized frequency f is between 0.15 and 0.32, the shape of the equal frequency line is approximately circular, which means that the light propagation in the two-dimensional hexagonal-square-lattice photonic crystal is similar to that in ordinary isotropic media [20]. Therefore, we can use the equivalent refractive index n_{eff} to represent the propagation of light in the crystal at this time.

The variation curve of the equivalent refractive index n_{eff} with the normalized frequency f can be obtained by the finite-difference-time-domain method, as shown in Fig. 3. It can be seen that $n_{\text{eff}} \leq 0$ when $0.15 \leq f \leq 0.32$, and $n_{\text{eff}} \cong -1$ when the corresponding normalized frequency $f \cong 0.251$. The normalized frequency of the light source we selected is 0.251, unless otherwise specified.

Resolution is an important parameter of the lens performance. By increasing the resolution of the target, we can easily optimize its performance. Imaging studies of small targets are still in their infancy, so it is necessary to study how to improve the resolution of the imaging system. In the simulation below, the frequency of the light source is 0.251 (a/λ), and an equivalent refractive index of the NR-PC flat lens is -1. Place light source at $(-\lambda, 0)$, the width of the NR-PC plate is $d = 2\,\lambda$ in the range of $0 \leq z \leq 2\,\lambda$, and the circular perfect electric conductor with radius $R = 1/12\,\lambda$. The target is placed at focus F_2 $(d_2 = 0.83\,\lambda)$, as shown in Fig. 4. In order to obtain the backscattered wave of the target, the light source is kept moving synchronously with the detector in the x axis direction (measured every 0.2 μm from -4 to 4 μm) at $z = -\lambda$. After the simulation experiment and numerical simulation, the total light-field-intensity map can be obtained; then the target is removed and rescanned once. The corresponding scattered-signal field strength of a circular PEC target can be calculated by the signal level value detected when the target exist subtracts the field strength value without target. For comparison, we normalize the scattered field strength from the target, that is, the maximum value of the scattered field strength is set to unit 1, and the remaining values are the ratio of the corresponding original field strength value to the maximum value.

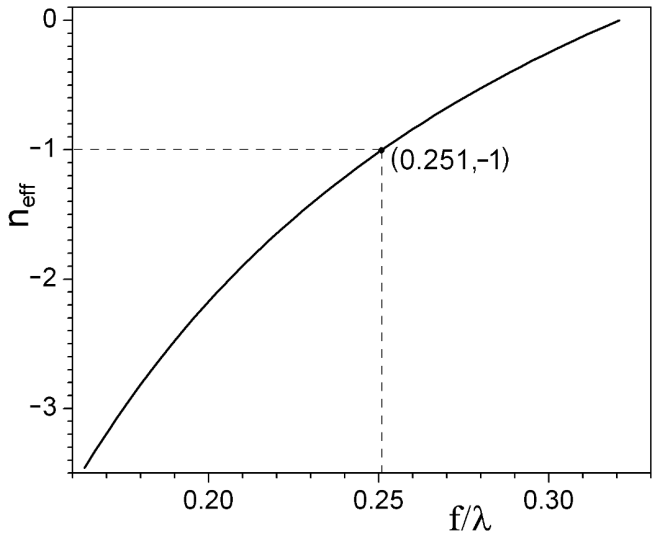

Fig. 3. Change curve of n_{eff} and f in the two-dimensional triangular NR-PC flat lens (TM mode).

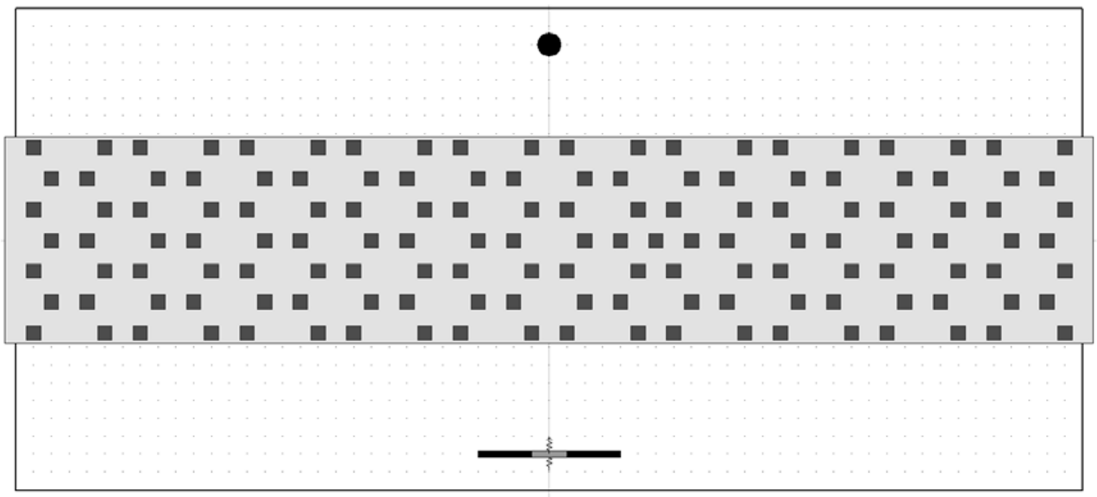

Fig. 4. The structure diagram of two-dimensional hexagonal-square-hole photonic-crystal flat lens.

3. Results and Analysis

In this paper, we define the resolution as the lateral width at 0.707 times the peak value of the field strength of the scattered signal [21]. In Fig. 5, we show the normalized field-strength distribution obtained with the two-dimensional hexagonal flat lens and without the lens. The resolution ($0.3486\,\lambda$) obtained with a two-dimensional hexagonal flat lens is much better than the resolution without the lens ($1.421\,\lambda$), and the resolution is improved by about four times. This is because the two-dimensional hexagonal flat lens has a focusing effect, which can focus the light wave of the light source at the target, generate a strong backscattered wave, and cause the backscattered wave to gather near the point source. Therefore, the focal resolution of the backscattered wave can be significantly improved.

Then we changed the side length of the air hole to study the effect of the side length on the imaging resolution of the system; the changes were from $0.1\,a$ to $0.5\,a$ with a variation interval of $0.1\,a$. The change of the side length first verifies whether the normalized frequency changes with the equivalent refractive index of -1. The simulation calculation shows that the normalized resolution of the side-length change remains unchanged at 0.251 (a/λ). The normalized frequency in the next simulation also does not change. The simulation results are shown in the following Fig. 6 and Table 1. As it was mentioned above, we define the resolution as the lateral width at 0.707 times the peak value of the field strength of the scattered signal. The figures near the curves in Fig. 6 are the coordinate values of the X axis corresponding to a normalized field strength of 0.707. The plots are bilaterally symmetric in the vicinity of $X = 0$, i.e., the value of resolution is the coordinate value of the X axis multiplied by 2.

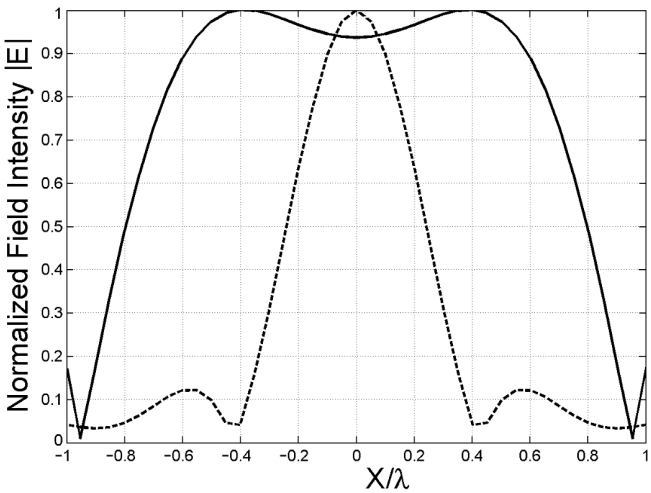

Fig. 5. The normalized field intensity of the scattering signal obtained with the NR-PC flat lens (solid curve) and without it (dashed curve).

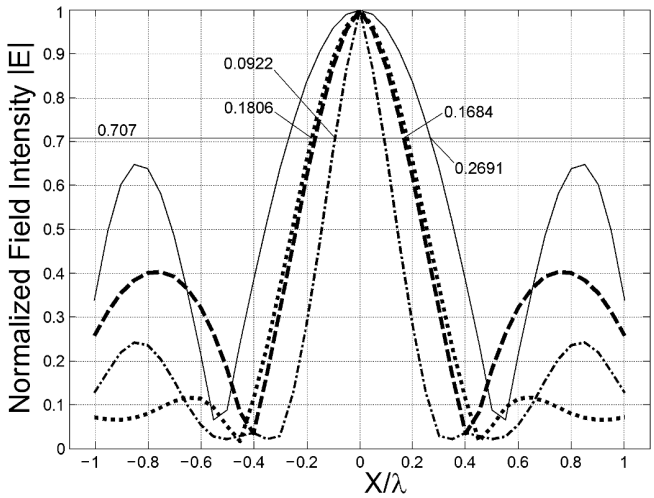

Fig. 6. The normalized field intensity of the scattering signal with different side lengths, i.e., $0.1\,a$ (solid curve), $0.2\,a$ (dashed curve), $0.3\,a$ (dotted curve), and $0.5\,a$ (dash-dotted curve).

Table 1. Comparison of the Refocusing Resolution of the NR-PC Flat Lens with Different Side Lengths.

Radius	$R = 0.1\,a$	$R = 0.2\,a$	$R = 0.3\,a$	$R = 0.4\,a$	$R = 0.5\,a$
Resolution	$0.5382\,\lambda$	$0.3368\,\lambda$	$0.3612\,\lambda$	$0.3486\,\lambda$	$0.1844\,\lambda$

In Fig. 6 and Table 1, one can see that resolutions for different side lengths are also different. A general

trend is that the resolution gradually increases with increase in the side length, and the resolutions for the side lengths $L = 0.2\,a$, $0.3\,a$, and $0.4\,a$ are approximately the same. The resolution at $L = 0.5\,a$ is the best and reaches $0.1844\,\lambda$; also the resolution is improved by 47% compared to that at $L = 0.4\,a$. As the length of the air hole increases, the proportion of the air hole area in the flat panel system increases, i.e., the periodicity increases, resulting in increase in the resolution of the system. Thus, one can see that the imaging resolution of the system can be optimized by changing the side length of the square air hole.

4. Conclusions

In this paper, we studied the near-field imaging resolution of a two-dimensional hexagonal-square air-hole flat-lens system by the plane-wave expansion method and the time-domain-finite-difference method. The simulation results show that the resolution of the lens system is greatly improved (about four times) compared with the absence of the flat lens due to the resonance excitation effect of the equivalent negative refraction [22,23] and the evanescent-wave-amplification effect [2]. Next, we study the effect of the length of the square air hole on the resolution of the system. The results show that the periodicity of the flat-lens system increases with increase in the air-hole length from $0.1\,a$ to $0.5\,a$ (interval $0.1\,a$). The more obvious that the general trend of resolution is getting higher and higher. The research performed has certain guiding significance for improving the detection ability of small targets and the practical application and optimization of photonic-crystal flat-lens systems.

Acknowledgments

This work was supported by grants from the Construction of Experiment Technician Team of Shanghai Higher-Education Institutions.

References

1. V. G. Veselago, *Sov. Phys. Usp.*, **10**, 509 (1968).
2. J. B. Pendry, *Phys. Rev. Lett.*, **85**, 3966 (2000).
3. J. T. Shen and P. M. Platzman, *Appl. Phys. Lett.*, **80**, 3286 (2002).
4. S. A. Cummer, *Appl. Phys. Lett.*, **82**, 1503 (2003).
5. X. S. Rao and C. K. Ong, *Phys. Rev. E*, **68**, 067601 (2003).
6. G. Wang, J. R. Fang, and X. T. Dong, *Opt. Express*, **15**, 3312 (2007).
7. G. Wang, J. R. Fang, and X. T. Dong, *IEEE Trans. Antennas Propag.*, **55**, 3534 (2007).
8. D. R. Smith, W. J. Padilla, D. C. Vier, et al., *Phys. Rev. Lett.*, **84**, 4184 (2000).
9. R. A. Shelby, D. R. Smith, and S. Schultz, *Science*, **292**, 5514:77-79 (2001).
10. E. Yablonovitch, *Phys. Rev. Lett.*, **58**, 2059 (1987).
11. S. John, *Phys. Rev. Lett.*, **58**, 2486 (1987).
12. C. Luo, S. G. Johnson, J. D. Joannopoulos, et al., *Phys. Rev. B*, **65**, 201104 (2002).
13. P. V. Parimi, W. T. Lu, P. Vodo, et al., *Nature*, **426**, 404 (2003).
14. Y. T. Fang, H. J. Sun, T. G. Shen, *Opt. Mater.*, **28**, 1156 (2006).
15. Y. T. Fang and T. G. Shen, *Chin. Phys. Lett.*, **22**, 949 (2005).
16. E. Yablonovitch, T. J. Gmitter, and K. M. Leung, *Phys. Rev. Lett.*, **67**, 2295 (1991).
17. F. Bloch, *Z. Physik*, **52**, 555 (1929).
18. K. S. Yee, *IEEE Trans. Antennas Propag.*, **14**, 302 (1966).

19. J. P. Berenger, *J. Comput. Phys.*, **114**, 185 (1994).
20. S. Foteinopoulou and C. M. Soukoulis, *Phys. Rev. B*, **72**, 165112 (2005).
21. R. D. Meade, A. M. Rappe, K. D. Brommer, et al., *Phys. Rev. B*, **48**, 8434 (1993).
22. A. Sharon, D. Rosenblatt, and A. A. Friesem, *Appl. Phys. Lett.*, **69**, 4154 (1996).
23. I. V. Shadrivov, A. A. Sukhorukov, Y. S. Kivshar, et al., *Phys. Rev. E*, **69**, O16617 (2004).